

Hydrogen storage system based on novel carbon materials and heat pipe heat exchanger

L.L. Vasiliev *, L.E. Kanonchik, A.G. Kulakov, V.A. Babenko

Luikoy Heat & Mass Transfer Institute, National Academy of Sciences, P. Brovka, 15, 220072, Minsk, Belarus

Received 15 October 2005; received in revised form 22 November 2006; accepted 27 November 2006

Abstract

Adsorbed hydrogen is being considered as a potential energy carrier for vehicular applications to replace compressed gas due to its high energy density capability. A new design of hydrogen storage vessel using novel carbon sorbents and heat pipes thermal control is the subject of research program oriented on 5–10 kg of hydrogen be stored on-board. Porous structure and hydrogen-sorption capacities of activated carbon materials are considered. Numerical analysis based on 2D nonequilibrium model of heat and mass transfer in the sorbent cylinder is carried out with the aim to investigate and optimize the sorption storage system. Obtained numerical and experimental data testify the possibilities of a new sorbent bed to reduce the operating pressure and increase a gas storage capacity.

© 2006 Elsevier Masson SAS. All rights reserved.

Keywords: Carbon; Methane; Hydrogen; Heat pipe; Sorption; Storage system

0. Introduction

It is known that nearly all of our vehicles currently run on either gasoline or diesel fuel, which is dangerous with the point of view of nature protection. This situation requires that alternative energy carriers to be developed to promote future energy security. Hydrogen and natural gas have the potential to be a very attractive alternative energy carrier. These two gases are clean, efficient, and derived from diverse domestic resources, such as fossil fuel. Success in development of a new hydrogen technologies, such as fuel cells, transport systems on hydrogen, metal hydride based heat pumps has shown, that the use of hydrogen and natural gas results in qualitatively new solutions of ecological and power problems. The advantage of hydrogen use is associated with ecological cleanliness. Hydrogen is free of toxic substances that are added, e.g. to gasoline to increase the octane number. Hydrogen is considered to be the most fire-safe kind of fuel in view of high temperature of ignition.

Among the disadvantages of hydrogen are its low density and small volume heat of combustion, which leads to the ne-

cessity of storing it in large-sized vessels and cylinders. According to the standard “the US department of energy (DOE) hydrogen plan” the modern onboard system of hydrogen storage should have capacity of storage 6–7 wt% at average pressure (2–6 MPa) and temperature 273–363 K; capacity of 5 kg, and specific energy of 7.2 MJ kg^{-1} . Current on-board hydrogen storage approaches involve compressed hydrogen gas tanks, liquid hydrogen tanks, metal hydrides, carbon-based materials, high surface area sorbents, and chemical hydrogen storage. None of the existing methods of hydrogen storage is dominant in terms of energy density, gas release rate, volume, and mass at same time [1]. From the practical point of view it is vital to find the most effective way to store hydrogen and then, to replace the current fuel systems. Each of the known hydrogen storage systems has its own advantages and disadvantages but does not provide the main goal—sufficient compactness.

One of ways of gradual penetration of hydrogen as a fuel for internal combustion engines is its application in dual-fuel vehicles (hydrogen–gasoline, hydrogen–methane) with a sorption system of gas storage. Such approach yields a minimum increase of weight at the expense of storage system and does not require application of electro motors, commutators, and heavy accumulators. In service of the dual-fuel motor transport

* Corresponding author. Tel./fax: +(375 17) 284 21 33.
E-mail address: lvasil@hmti.ac.by (L.L. Vasiliev).

Nomenclature

a	adsorption capacity	kg kg^{-1}	V_g	molar gas-phase volume
a_v	volume capacity of hydrogen storage using physisorption	ml(STP) g^{-1}	z_g	coefficient of gas compressibility
c	density of free gas	kg m^{-3}	<i>Greek letters</i>	
C	solid sorbent specific heat capacity . . .	$\text{J kg}^{-1} \text{K}^{-1}$	α	heat transfer coefficient $\text{W m}^{-2} \text{K}^{-1}$
C_g	specific heat capacity of free gas	$\text{J kg}^{-1} \text{K}^{-1}$	ε	porosity determined as a part of the volume occupied by the free gas (not bound by adsorption)
C_a	specific heat capacity of adsorbed gas . .	$\text{J kg}^{-1} \text{K}^{-1}$	2δ	fin thickness m, mm
E	activation energy	J kg^{-1}	λ	effective thermal conductivity of the sorbent layer $\text{W m}^{-1} \text{K}^{-1}$
G	gas output from the cylinder	$\text{kg sec}^{-1}, \text{g sec}^{-1}$	ρ_s	density of the solid sorbent kg m^{-3}
g_i	gas output from the elementary cell, used for computer modeling	kg sec^{-1}	ρ	total density of the free and adsorbed gases in the cylinder kg m^{-3}
K_{s0}	pre-exponent constant in the equation of kinetic of sorption	s^{-1}	ρ_v	volume density of storage ml(STP) ml^{-1}
M	mass of the gas in the cylinder	kg	τ	time sec
M_i	mass of the gas in the calculated cell	kg	<i>Subscripts</i>	
m	dynamic coefficient of filling the cylinder		a	adsorbate
N	number of calculated cells in the cylinder		cr	critical state
P	pressure	Pa	e	finite value
q_{st}	latent isosteric heat of sorption	J kg^{-1}	env	environment
Q	heat flow	W	eq	equilibrium conditions
r and z	cylindrical coordinates	m	hp	heat pipe
R	external radius of the cylinder shell	m	0	initial value
R_0	internal radius of the heat pipe	m	s	sorbent
r_0 and r_1	internal and external radii of the annular layer of the sorbent	m	f	fin
R_μ	gas constant	$\text{J kg}^{-1} \text{K}^{-1}$	t	transfer
R_p	mean radius of the particles	mm	<i>Abbreviations</i>	
$2S$	fins step	m, mm	SSSG	sorption storage system of gas
T	temperature	K, °C	HE	heat element
W_0	maximum microporous specific volume . .	$\text{m}^3 \text{kg}^{-1}$	HP	heat pipe
v	component of the velocity vector	m sec^{-1}	STP	standard of temperature (273 K) and pressure (0.1 MPa)
v_a	specific volume of adsorbed medium . . .	$\text{m}^3 \text{kg}^{-1}$		
V_a	partial molar adsorption volume			

a change is possible from hydrogen fuel to hydrocarbon fuel or to their mixture, depending on accessibility of this or that fuel. An application of combined (hydrogen and methane) gas storage systems is promising as an alternative. Besides natural gas is a potential source for large scale production of pure hydrogen as a result of catalytic conversion of methane. In the fuel cell automobile hydrogen can be disposed in container in the adsorbed state or made immediately from accumulated methane.

Realization of any scheme of hydrogen usage in transport depends on making a cost-effective system of gas storage. Successful development of a getter system of hydrogen storage presumes a presence of an active thermal regulation and special properties of materials capable to store up hydrogen efficiently. Alongside with a large total yield of hydrogen the high density of energy storage is required for minimization of volume and/or a system weight. Ranges of pressure and temperatures should also correspond to service conditions on transport.

Liquid hydrogen tanks can store more hydrogen in given volume than compressed gas tanks, since the volumetric capac-

ity of liquid hydrogen is 0.070 kg l^{-1} . Advantage of sorption hydrogen storage in cryogenic tanks containing sorbents, as contrasted to the storage of compressed and metal hydrides absorbed hydrogen is that an amount of stored hydrogen per unit of mass is more. Besides, the cost of mass unit of sorbent is lower, than the cost of mass unit of the metal alloys used for hydrogen storage [2]. Therefore, carbon with its low atomic mass can promote overcoming of these inconveniences. Microporous active carbon adsorbs hydrogen molecules and keeps them by surface intermolecular forces. But at the room temperature these forces are weak, as they are hindered from thermal agitation of molecules. To store considerable amounts of hydrogen, the carbon samples should be cooled down to cryogenic temperature. However, in most cases the cryogenic hydrogen storage system is economically unprofitable. The density of energy storage depends on porosity and properties of carbon surface. Even the energy capacity of storage is high, the bulk density of sorbents is low. An essential shortage of this mode is the necessity to use special heat-insulating, hermetic containers

to keep a cryogenic temperature. Hence, it is necessary to select microporous carbon sorbents, capable to retain hydrogen at low and room temperatures in the middle pressure range [3,4].

Since sorption procedure represents an exothermic and endothermic process, every final rate of adsorption or desorption is related to the temperature changes in the sorbent bed. Theoretical and experimental investigations [5–8] have shown that the value of sorption heat has a particularly significant effect during the desorption stage of sorbent bed. The rate of gas extraction from the storage vessel is determined by the rate of the fuel consumption of the vehicle. The advanced thermal control system based on heat pipes is efficient procedure combined with the gas accumulator to ensure the steady state of gas consumption by the vehicle.

Special features of the thermodynamic processes of gas adsorption and desorption are described by the equation of equilibrium state $a_{eq} = a_{eq}(P, T)$ and the equation of sorption kinetic determining the rate of the sorption capacity a approaching to its equilibrium value $a_{eq}(P, T)$. According to the equation of state, the lower the mean temperature of the sorbent, the larger nonrecoverable mass of gas $M_e \sim a(P_e, \bar{T}_e)$ remains in the vessel. The heat of exhausted gases or liquid system of motor cooling can be used to stimulate the gas release from the vessel. The process of gas extraction from a constant-volume vessel occurs at variable pressure, temperature, and gas mass. The pressure regulator at the outlet of cylinder provides the required gas flow rate, which depends on the velocity of vehicle and other conditions of its motion. In order to fulfill the requirements of economical efficiency and safety, the characteristics of the cylinder should be optimized.

This work is devoted to development and research of the thermally regulated onboard system of hydrogen and methane storage applying the novel carbon sorbents. Textural characteristics and sorption capacities of microporous carbon materials were experimentally determined. To improve the parameters of the gas storage systems the enhancement technology of carbon sorption capacity including additional activation was applied. Mathematical modeling of processes of charge and discharge for a sorption cylinder with finned heater/cooler was carried out. A two-phase heat exchanger (HE) as a heat pipe was used as an alternative to a single-phase heat exchanger, or electric heater. The heat pipe (or thermosyphon) has advantages over the other devices, since it permits using different kinds of energy (gas flame, electricity, steam, liquid).

1. Mathematical model

The analyzed element of the sorbent bed (SSSG) (Fig. 1) is bounded by the envelope ($r = R$) of the vessel, the wall of the finned HE ($r = R_0$), and the planes of symmetry passing through the center of the fin ($z = 0$) and the center of the sorbent bed ($z = S$) between two neighboring fins. The free gas fills the macro-pores, while the adsorbed gas is disposed on the micro-pores surface. The metal fin 1 (disk) with a half-width δ is attached to the outer wall 3 of the HE. The annular sorbent bed 2 with radii r_0 and r_1 is adjacent to the fin of the HE. The contact thermal resistance of HE with the microporous sorbent

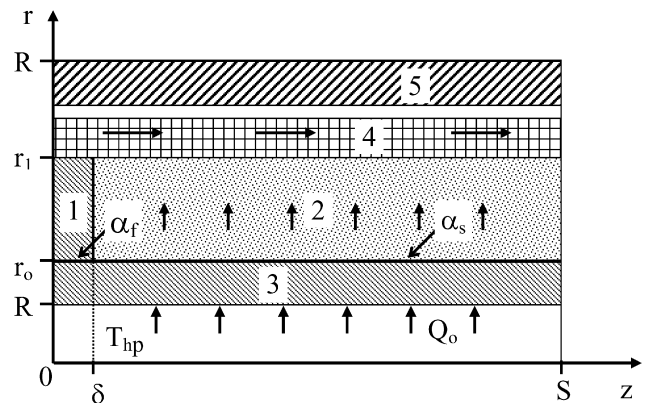


Fig. 1. Diagram of the calculated element of the SSSG: 1—fin; 2—sorbent; 3—shell of the heat pipe; 4—channel for gas output formed by the perforated tube and the cylinder body; 5—cylinder body.

is characterized by the heat transfer coefficient α_s . Analogous contact thermal resistances, but different in magnitude, can exist between the fin and the sorbent bed (α_{fs}), as well as between the fin and the outer surface of the HE (α_f).

The sorbent bed is surrounded by a thin perforated aluminum tube served for the gas release during its desorption from the sorbent bed. Since the thickness of the sorbent bed is much smaller than its length, the desorbed gas moves mostly in the radial direction. There is the channel 4 between the perforated tube and the vessel wall through which the gas moves along the cylinder to the pressure regulator. The gas flow rate is maintained constant with the help of pressure regulator. This factor, as well as the factor of heating/cooling of the sorbent bed, determines the rate and character of a pressure change in the vessel. During the period of gas release the vessel is cooled by the air convection (temperature T_{env}) with the coefficient of heat transfer α_{env} and is heated inside with heat pipe. Depending on the conditions of the sorbent bed heating, a constant temperature or heat flow is maintained at the inner surface of the HE. There is an assumption—all sorbent elements between the HE fins are under the same conditions. The resulting dependences for the sorbent bed can be obtained by simple summing over N identical elements.

The mathematical model of the gas vessel filled with a sorbent bed and gas is based on the following simplifying assumptions:

- (1) the pressure is practically uniform and the momentum equation becomes redundant; it means, that the characteristic pressure differences inside a cylinder are much less than general pressure drop between a cylinder and environment;
- (2) the resistance to the mass diffusion is small;
- (3) at each point of the vessel the temperature of the solid phase and the gas phase is the same, due to the high volumetric coefficient of heat transfer between them;
- (4) the free gas in the vessel is ideal;
- (5) the heat energy during the compressing or expanding gas is not taken into account;
- (6) gas is flowing in the radial direction through the sorbent bed.

In accordance with the assumptions, the model of heat and mass transfer in the sorbent bed is described by the energy equation, the equation of mass balance, the approximate kinetic equation, and the equation of equilibrium state (equation of isothermal adsorption).

1.1. Equation of isothermal adsorption

The adsorption properties of activated carbons are determined with accuracy sufficient for practical purposes by the potential theory of adsorption developed in [9]. Physisorption on microporous carbons can be described with the Dubinin–Radushkevich equation:

$$a = \frac{W_0}{v_a} \exp \left\{ - \left[\frac{R_\mu T \ln(P_{\text{sat}}/P)}{E} \right]^2 \right\} \quad (1)$$

Equilibrium state equation (1) includes the saturation pressure P_{sat} . Since the hydrogen sorption isotherms are measured within the temperature and pressure intervals comprising the regions of supercritical states ($T_{\text{cr}} = 33.24$ K, $P_{\text{cr}} = 1.298$ Pa), the notion of saturation pressure loses its physical meaning. In the work [10] the saturation pressure is determined by the formula:

$$P_{\text{sat}} = P_{\text{cr}}(T/T_{\text{cr}})^2 \quad (2)$$

1.2. Approximate kinetic equation

Many authors [11–14] have mentioned that any finite rate of sorption is associated with the temperature changes in the sorbent volume. Therefore, in the mathematical model formulation it is necessary to take into account the fact that a sorption is nonequilibrium process. High rates of desorption of molecules from microporous adsorbents are the necessary condition of the efficient operation of the SGSS on vehicles. For the reason, the SGSS needs to be calculated with consideration its kinetic characteristics. The process of desorption of molecules from bidispersed adsorbents such as activated carbons involves the following stages: escape of adsorbate molecules from the active centers on the adsorbent surface, diffusion of molecules in the initial porous structure, diffusion in secondary pores, and removal of the desorbate molecules from the gas phase.

Estimation of the contribution of the rate of individual processes to the total rate of desorption, performed on the basis of the analysis of experimental data, has shown [15] that the velocity of molecular escape from the adsorbent surface is of crucial importance. The rate of mass transfer in adsorbent granules increases due to the migration of molecules over the surface of the pores. This transfer is given the name surface diffusion. In practice, the dynamics of sorption is described by the Gluckauf equation [16], in which the motive force of the intradiffusion adsorption process is determined as the difference of the adsorbate concentrations in the solid phase:

$$\frac{da}{d\tau} = \beta_k(a_{\text{eq}} - a) \quad (3)$$

where β_k is the kinetic coefficient.

Sakoda et al. [17–19] recommend to assume, that the kinetic coefficient β_k in the approximate equation of the kinetics of

sorption on activated carbons is equal to the total coefficient of mass transfer $\beta_t = 15D_s/R_p^2$.

The coefficient of surface diffusion D_s in a microporous sorbent is related to the temperature by the dependence $D_s = D_{s0} \exp[E/(R_\mu T)]$, where D_{s0} is a phenomenological constant.

For the sorption processes of filling of the SSG with a gas and its discharge, we use the kinetic equation in the form [20]

$$\frac{da}{d\tau} = K_{s0} \exp \left(- \frac{E}{R_\mu T} \right) (a_{\text{eq}} - a) \quad (4)$$

where $K_{s0} = 15D_{s0}/R_p^2$.

Thus, to describe the nonequilibrium desorption occurring during the discharge of a cylinder, it is necessary to use two equations. One of them (1) describes the dependence of the equilibrium value of the adsorption a_{eq} on the pressure and temperature, and the other (4) describes the time by which the nonequilibrium adsorption is occurred behind the equilibrium one a_{eq} . The relation of the magnitude of the adsorption a to the pressure in Eq. (4) is considered as the dependence of a on $a_{\text{eq}}(P, T)$.

1.3. Continuity equation

The total density ρ' of the free and the adsorbed gases in the cylinder is expressed as $\rho' = \varepsilon c + \rho a$. In accordance with the assumptions made, the continuity equation for a cylindrical sorbent layer has the form

$$r \frac{\partial}{\partial \tau} (\varepsilon c + \rho a) + \frac{\partial}{\partial r} (rcv) = 0 \quad (5)$$

During the time of desorption of the sorbent bed the pressure in the cylinder is increasing and its value depend on the integral mass balance condition. The total mass of the gas in the calculated sorbent element (Fig. 1) is determined by the integral $M_i = 2\pi \int_\delta^s \int_{r_0}^{r_1} (\varepsilon c + \rho a) r dr dz = M/N$ and the mass rate of the gas discharge out of the element $g_i = G/N$ is given by expression

$$\frac{dM_i}{d\tau} = -g_i \quad (6)$$

The density of free gas \tilde{n} is found from the equation for the ideal gas:

$$c = \frac{P}{R_\mu T} \quad (7)$$

Differentiating (7) with respect to time, we write

$$\frac{dc}{d\tau} = c \left(\frac{\partial \ln P}{\partial \tau} - \frac{\partial T}{T \partial \tau} \right) \quad (8)$$

Substitution of the derivatives $\frac{dc}{d\tau}$ and $\frac{da}{d\tau}$ from (4) and (8) into (6) gives the equation

$$2\pi \int_\delta^s \int_{r_0}^{r_1} \left(\varepsilon c \left(\frac{d \ln P}{d\tau} - \frac{\partial T}{T \partial \tau} \right) + \rho K_{s0} \exp \left(- \frac{E}{R_\mu T} \right) (a_{\text{eq}} - a) \right) r dr dz = -g_i \quad (9)$$

From this equation, we can determine the rate of the pressure change in the vessel:

$$\frac{d \ln P}{d\tau} = (I_2 - I_3 - g_i)/I_1 \quad (10)$$

where

$$\begin{aligned} I_1 &= 2\pi \int_{\delta}^s \int_{r_0}^{r_1} \varepsilon c r dr dz \\ I_2 &= 2\pi \int_{\delta}^s \int_{r_0}^{r_1} \frac{\varepsilon c}{T} \frac{\partial T}{\partial \tau} r dr dz \\ I_3 &= 2\pi \int_{\delta}^s \int_{r_0}^{r_1} \rho K_{s0} \exp\left(-\frac{E}{R_\mu T}\right) (a_{\text{eq}} - a) r dr dz \end{aligned} \quad (11)$$

1.4. Equation of energy balance

The equation of the heat energy balance for a sorbent material in the cylindrical coordinate system can be written as:

$$\begin{aligned} r(\varepsilon c C_g + \rho C + \rho a C_a) \frac{\partial T}{\partial \tau} + r c v C_g \frac{\partial T}{\partial r} \\ = \frac{\partial}{\partial r} \left(r \lambda_{\text{eff}} \frac{\partial T}{\partial r} \right) + \frac{\partial}{\partial z} \left(r \lambda_{\text{eff}} \frac{\partial T}{\partial z} \right) + r q_{\text{st}} \rho \frac{\partial a}{\partial \tau} \end{aligned} \quad (12)$$

The heat of the phase transition of sorption can be calculated using Clausius–Clapeyron equation with some corrections. In accordance with [21], the isosteric sorption heat of a gas mole is determined by the formula

$$q_{\text{st}} = \left(1 - \frac{V_a}{V_g} \right) T R_\mu z_g \left[\frac{\partial \ln P}{\partial \ln T} \right]_{a=\text{const}} \quad (13)$$

For the ideal gas ($z_g = 1$, $V_a \ll V_g$), the isosteric heat is calculated from the relation

$$q_{\text{st}} = R_\mu T \left[\frac{\partial \ln P}{\partial \ln T} \right]_{a=\text{const}} \quad (14)$$

The limits of applicability of Eq. (14) are depend on the degree to which the gas can be approximated as ideal, i.e., on the ratio between the partial molar volumes of the adsorbate and gas and on the compressibility coefficient. In the case of a nonideal gas, the estimation obtained with (2) should be considered as being approximative.

Note that in the left-hand side of Eq. (12) the term corresponding to the axial convective motion of the gas in the porous media is absent. The variable radial velocity component can be determined from the continuity equation (5). Eq. (5) is integrated over r , what gives

$$r v c = - \int_0^r \frac{\partial \rho'}{\partial \tau} r dr \quad (15)$$

According to (4) and (8) the size of $\frac{\partial \rho'}{\partial \tau}$ can be expressed through other functions. For simplification of expression (15) an additional assumption on self-similarity of time dependences of ρ' was taken:

$$\begin{aligned} r v c &= - \int_0^r \frac{\partial \rho'}{\partial \tau} r dr \approx - \frac{\int_0^r \rho' r dr}{\int_0^{r_1} \rho' r dr} \frac{d}{d\tau} \left(\int_0^{r_1} \rho' r dr \right) \\ &= \frac{g_i}{M_i} \int_0^r \rho' r dr \end{aligned} \quad (16)$$

Rearrangement of (12) together with (1) and (4)–(9) and (15) gives the equation of heat balance in the form

$$\begin{aligned} r \rho (C + a C_a) \frac{\partial T}{\partial \tau} \\ = \frac{\partial}{\partial r} \left(r \lambda_{\text{eff}} \frac{\partial T}{\partial r} - \frac{g C_g T}{M} \int_0^r \rho' r dr \right) \\ + \frac{\partial}{\partial z} \left(r \lambda_{\text{eff}} \frac{\partial T}{\partial z} \right) - r c T C_g \frac{d \ln P}{d\tau} \\ + r q'_{\text{st}} \rho K_{s0} \exp\left(-\frac{E}{R_\mu T}\right) (a_{\text{eq}} - a) \end{aligned} \quad (17)$$

where $q'_{\text{st}} = q_{\text{st}} - T C_g$. In this equation, the effects of the non-equilibrium sorption and the existence of the free gas in the cylinder are taken into account. The influence of the sorption heat is modeled by additional contribution to the heat capacity of the system and the source term in the right-hand side of the equation, related to the pressure change. Thus, the equation of equilibrium state (1), the kinetic equation (4), the equation of heat balance (17), and Eq. (10) describing the rate of the pressure change in the vessel in accordance with the integral law of conservation of mass form the complete system of functional equations for determining the variables T , P , a .

1.5. Initial and boundary conditions

In calculations we assumed that at the initial stage of the process of gas desorption the pressure and temperature are: $P|_{\tau=0} = P_0$ and $T(r, z)|_{\tau=0} = T_0(r, z) = T_{\text{env}}$. The pressure and the temperature determine the initial mass of gas in the vessel M_0 and, correspondingly, the initial mass in the calculated cell.

The boundary conditions were set for four surfaces (Fig. 1):

$$\frac{\partial T}{\partial z} \Big|_{z=0} = 0, \quad \frac{\partial T}{\partial z} \Big|_{z=S} = 0 \quad (18)$$

$$-\lambda \frac{\partial T}{\partial r} \Big|_{r=R} = \alpha_{\text{env}} (T - T_{\text{env}}) \quad (19)$$

$$-\lambda \frac{\partial T}{\partial r} \Big|_{r=R_0} = \frac{Q_{\text{hp}}}{2\pi R_0 S N} \quad \text{or} \quad T|_{r=R_0} = T_{\text{hp}} \quad (20)$$

The first condition (20) corresponds to the situation, where the heat flow Q_{hp} is known, and the second condition corresponds to the situation, where the heat flow is not limited, and the temperature T_{hp} is known. This temperature is maintained at the inner surface of the heat pipe due to the contact of its evaporation zone with a large heated body, such as an engine.

For solution of the formulated mathematical model with the initial and boundary conditions, we used the method of finite

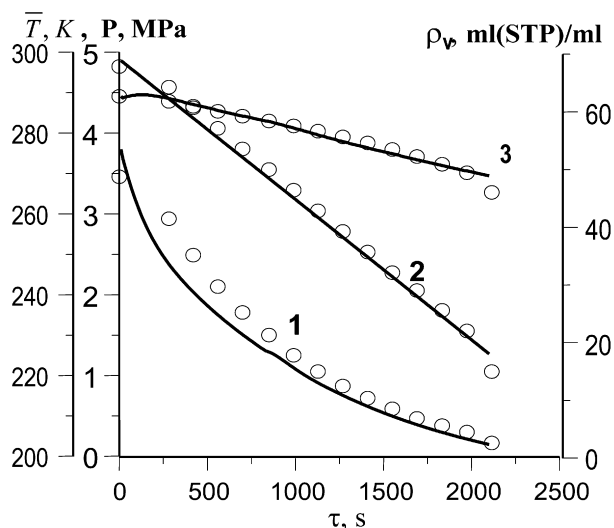


Fig. 2. Experimental points and calculated curves of the values of the mean temperature of the sorbent (3), the pressure (1), and the volume storage density of methane (2) as functions of time in the process of discharge of the SSSG.

elements [22] on a fixed grid. The typical number of triangular elements in the calculated region was from 200 to 300. Convergence precision was equal to 10^{-6} . For control of numerical errors the test calculations at different grids and time steps have been carried out. The system of equations with a sorption source is stiff and allows integration only with a small time step. For achievement of required accuracy and numerical stability the integration step did not exceed 2 s.

To verify the reliability of the mathematical modeling we compared the results of the calculations with the experimental data on the desorption methane [20] obtained at the Luikov Institute. A cylinder of volume 12.5 liters was tested at an ambient temperature $T_{\text{env}} = 290$ K and the constant heat flow Q_{hp} . As a sorbent material, commercially available activated carbon fiber “Busofit-AYTM” was used. In this case, the gas flow rate 0.2 g sec^{-1} was considered. Fig. 2 presents the dynamics of the mean-volume temperature, the pressure, and the volume storage density change of the sorbent bed for the heat flow $Q_{\text{hp}} = 80$ W

($G = 0.2 \text{ g s}^{-1}$). All the basic numerical parameters of the discharge process agree satisfactorily with the experimental data, Fig. 2.

2. Experimental data of the hydrogen-sorption capacity for the activated carbon materials

Hydrogen storage by solid materials is considered in [23]. Initially the research was based on cryogenic systems [24], which are unprofitable from the economical point of view. Recently the studies have focused on the search of the high capacity adsorbent to be used at room temperature [25]. For conventional activated carbon, the hydrogen uptake is proportional to its surface area and pore volume, while, unfortunately, a high hydrogen adsorption capacity (4–6 wt%) can be only obtained at cryogenic temperature according to theoretical calculations. To gain the goal of the problem—efficient methane and hydrogen storage and transportation it is necessary to develop a high performance microporous adsorbent material and an advanced system of the vessel thermal control.

The activated carbon fiber “Busofit” and activated wood-based carbon particles (the Institute of General and Inorganic Chemistry, NASB) fabricated in Belarus are considered as perspective materials for gas storage systems (Fig. 3), [26]. A new type of microporous material “Busofit”, product of pyrolyzed cellulose, is in the form of an active carbon fiber disks. It is considered as an advanced sorbent material, capable of delivering near 170 volumes of methane per volume of the vessel at pressure 3.5 MPa. The carbon fiber “Busofit” can be considered as a universal microporous adsorbent with pore diameter of 1–2 nm and at the same time as a material with high gas permeability. Impregnated cellulose—containing raw for manufacture special activated carbon materials for methane and hydrogen storage systems with high micro porosity, surface area and narrow micropore size distribution is the attractive host material for adsorption of different gases. A test matrix was assembled from 10 different carbon samples (additionally activated in the Luikov Institute and commercially available), including activated carbon fibers “Busofit” and granular activated carbons.

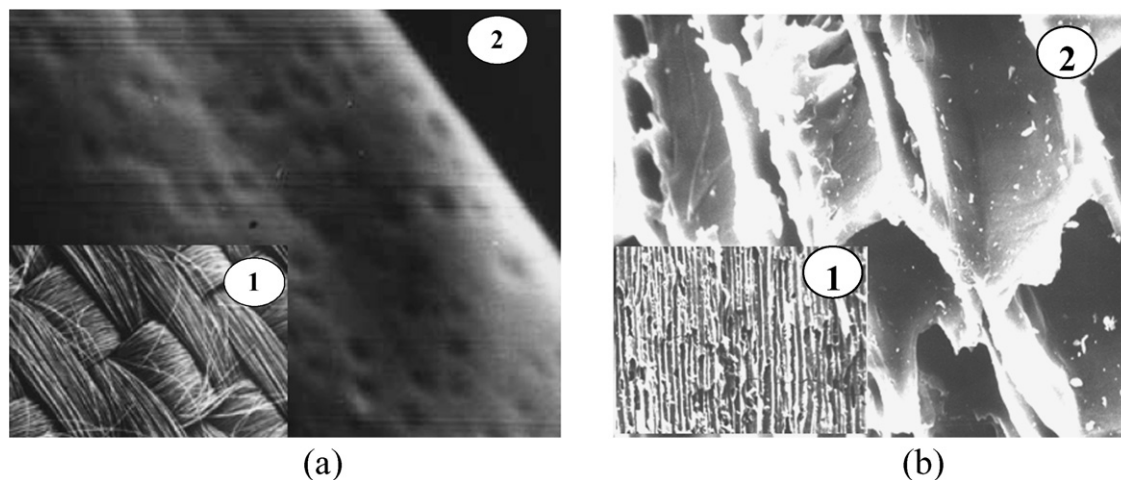


Fig. 3. Texture of novel carbon materials: (a) active carbon fiber “Busofit” (1—image multiplied by 50 times; 2—by 25 000 times); (b) active carbon material (IGIC NASB) made from waste wood (1—image multiplied by 30 times; 2—1000 times).

Table 1
Textural characteristics and hydrogen-sorption capacities at 77 K and 0.1 MPa for the investigated active carbon materials

No.	Sorbent	a_v , ml(STP) g ⁻¹	a_H , g g ⁻¹	S_H , m ² g ⁻¹	S_{BET} , m ² g ⁻¹	S_{DR} , m ² g ⁻¹	V_{DR} , ml g ⁻¹	$R_{DR} \times 10^8$, m
1	Busofit 191-5	199.9	0.0176	462	1691	2496	0.887	49.9
2	Busofit-M2	203.9	0.0179	465	1702	2507	0.89	41.5
3	Busofit-M4	225.1	0.0198	536	1715	2547	0.9	42
4	Busofit-M8	252.9	0.0223	571	1939	2985	1.04	51
5	WAC 97-03	115	0.0101	271	715	1050	0.37	33.4
6	WAC 19-99	172.1	0.0151	393	1005	1486	0.53	41.7
7	WAC 3-00	221.1	0.0195	575	1383	2142	0.74	50
8	207C	209.2	0.0184	502	1300	1944	0.69	41
9	Norit sorbonorit-3	193.8	0.0171	458	1361	2044	0.73	50
10	Sutcliff	236.6	0.0208	527	1925	2864	1.02	53.6

Note: WAC—wood-based active carbon; a_v —volume capacity of hydrogen storage using physisorption; a —capacity of hydrogen storage using physisorption; S_H —BET surface area determined on hydrogen; S_{BET} —BET surface area determined on nitrogen; S_{DR} —surface area, determined on Dubinin–Radushkevich method; V_{DR} —micropore volume, determined on Dubinin–Radushkevich method; R_{DR} —size of pore, determined on Dubinin–Radushkevich method.

Table 2
Textural characteristics and hydrogen-sorption capacities at 77 K and 0.1 MPa for carbonaceous materials [25]

No.	Sorbent	S_{BET} , m ² g ⁻¹	V_{DR} , ml g ⁻¹	a_v , ml g ⁻¹	$a_{v,meso}$, ml g ⁻¹	$a_{v,micro}$, ml g ⁻¹
1	Synthetic graphite	7	0.00	0	0	0
2	Large-diameter CNF	49	0.01	6	2	4
3	Activated graphite 100	119	0.02	14	6	8
4	Medium-diameter CNF1	120	0.00	12	11	1
5	ACF 400	883	0.34	143	1	142
6	ACF 1200	899	0.37	184	1	183
7	AC Norit 990721	988	0.43	142	2	140
8	AC Norit ROZ 3	287	0.05	36	6	28
9	Activated graphite 300	287	0.05	36	16	19
10	Medium-diameter CNF2	65	0.00	7	7	0
11	AC Norit SX 2	841	0.27	150	17	133
12	ACF 500	988	0.40	142	15	127
13	AC Norit UOK A	1195	0.47	188	10	178
14	AC Norit SX 1	922	0.31	168	18	150
15	AC Norit SX 1G AIR	1030	0.36	171	16	155
16	AC Norit GSX	933	0.26	161	27	134
17	AC Norit SX plus	1051	0.35	165	21	144
18	AC Norit SX 1 G	1176	0.40	187	20	167
19	AC Norit 990293	2029	0.92	238	7	231
20	AC Norit Darco KB	1462	0.42	146	54	92
21	Hyperion CNF	238	0.00	22	22	0

The nitrogen and hydrogen sorption isotherms were measured with the High Speed Gas Sorption Analyser NOVA 1200 at 77 K in the pressure range 0–0.1 MPa. In our experiments four samples of carbon “Busofit-AYTM” (1–4) and three samples of wood-based activated carbon (5–7) obtained by new technology were investigated. The activated carbon 207C (8) was produced from coconut shell. Samples 9 and 10 corresponded to granular activated carbons, specially developed for methane storage. Some samples from “Busofit-AYTM” have been prepared by selective thermal processing at high temperature near 850 °C. In this way, some of the carbon atoms are removed by gasification, which yields a very porous structure. Numerous pores, cracks were formed in the carbon material increasing a specific surface area due to the growth of micropore volume. Additional activation of a sample 1 was carried out at the presence of oxygen. As follows from Table 1 the increase of time of activation from two hours up to eight hours in an atmosphere of carbonic gas promotes increase to sorption capacity almost in 1.5 times (samples 2 and 4). The atmosphere of carbonic gas appeared

more preferably oxygen for growth of a specific surface and sorption capacity—time of activation of samples 1 and 2 was identical. To increase the adsorption capacity and the bulk density of material we compressed active carbon fiber together with a binder. Briqueted “Busofit” disks have a high effective thermal conductivity and a large surface area. Wood-based carbons (5–7) were produced by controlled pyrolysis of waste wood and special activation.

Our results of the N₂ and H₂ physisorption measurements are summarized in Table 1. The experimental database of group of institutes—Inorganic Chemistry and Catalysis, Debye Institute, Utrecht University [25] are shown in Table 2 (CNF is used to designate carbon nanofibers, ACF is used for activated carbon fibers and AC for activated carbon). The sorbents were chosen to represent a large variation in surface areas and micropore volumes.

As it is seen, “Busofit-M8” has the highest values of a surface area and micropore volume among carbon fibrous materials. The granular carbon material “WAC 3-00”—“Sutcliff”

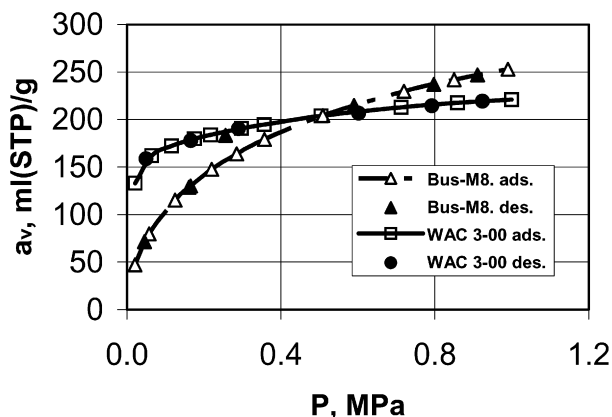


Fig. 4. Isotherms of hydrogen adsorption and desorption on carbon materials at temperature 77 K, measured by the high speed gas sorption analyser NOVA 1200.

made from wood-based activated carbons it also considered as a good sorbent media. “Busofit-M8” and “Sutcliff” have micropore volume more than 1 ml g^{-1} . They are also the best storage systems for hydrogen (accordingly $253 \text{ ml(STP) g}^{-1}$ and $237 \text{ ml(STP) g}^{-1}$) storage. The results obtained demonstrate that a large capacity of adsorbed hydrogen by physisorption under chosen conditions is valid for the sorbent bed containing a large volume of micropores and a high BET surface area. If we combine the carbon material with metal hydride/chloride microcrystals disposed in the same volume, we can solve the problem of efficient gas storage and transportation. Optimization of sorbent materials and sorption conditions is expected to lead to a hydrogen storage capacity of $500\text{--}600 \text{ ml(STP) g}^{-1}$, close to targets set for mobile applications.

Fig. 4 shows the experimental isotherms of the hydrogen adsorption and desorption on carbon fiber “Busofit-M8” and wood-based activated carbon “WAC 3-00” at the nitrogen tem-

Table 3

The empirical coefficients of Dubinin–Radushkevich equation for hydrogen sorption on the carbon materials

Material	$W_0 \times 10^3, \text{ m}^3 \text{ kg}^{-1}$	$E, \text{ kJ kg}^{-1}$
Busofit-M2	369	1783
Busofit-M4	376	1922
Busofit-M8	482	1710
Sutcliff	453	1699
WAC 3-00	270	3782
207C	343	1969

perature. Absence of an appreciable hysteresis confirms that reversible physisorption exclusively takes place with all investigated materials. As a result of the experiments, we obtained hydrogen sorption isotherms for different carbon materials and empirical coefficients for the Dubinin–Radushkevich equation (3), presented in Table 3.

There is a general need to have a good fit of experimental isotherms and temperature and to extrapolate some isotherms beside the experimental field. Fig. 5 compares the behaviour of the adsorption isotherms at different temperature levels for steam activated “Busofit-M8” and wood-based carbon “WAC 3-00”.

3. Results of the numerical investigation

The suggested simple model gives us a possibility to obtain the 2D fields of temperature and gas concentrations during charge-discharge (adsorption/desorption) procedure and investigate on this ground the efficiency of the gas vessel.

A set of calculations was performed for the high-surface area activated carbon fiber “Busofit-M8” and wood-based carbon “WAC 3-00” as promising gas sorption materials to design a hydrogen storage system. During gas discharge of the ves-

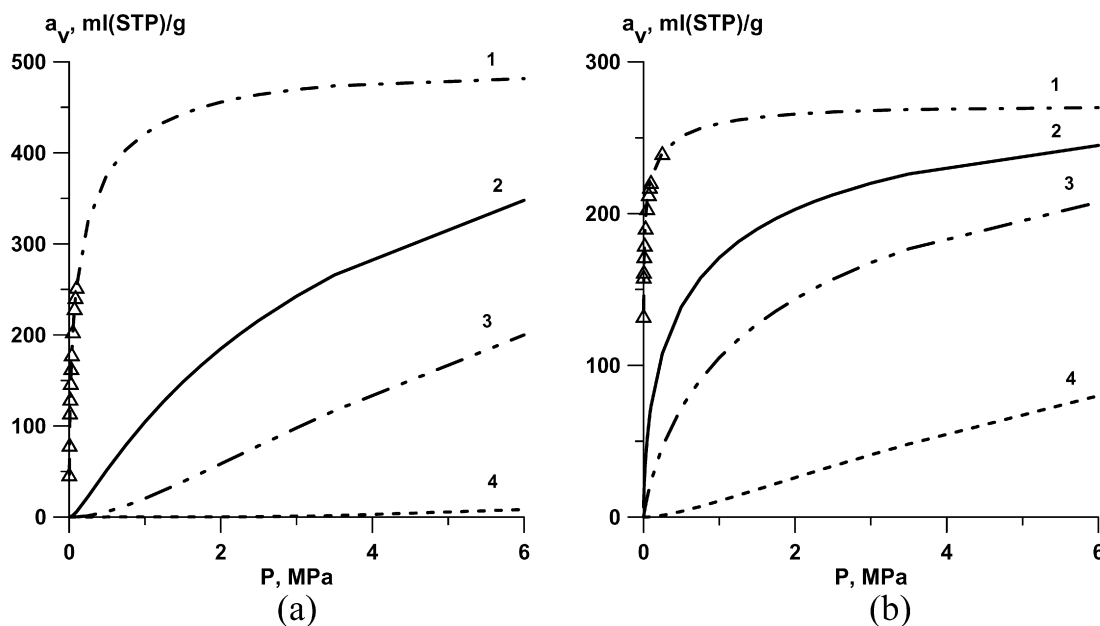


Fig. 5. Hydrogen adsorption isotherms for active carbon fiber “Busofit-M8” (a), wood-based carbon “WAC 3-00” (b) at different temperatures (1—77 K, 2—153 K, 3—193 K, 4—293 K): experimental data—points, calculated data (Dubinin–Radushkevich equation)—lines.

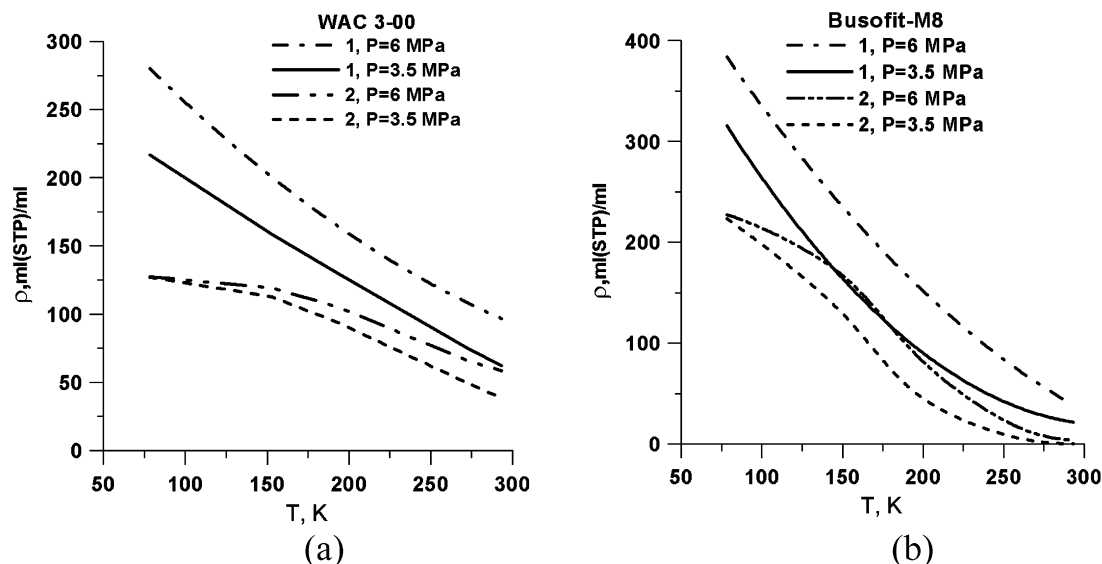


Fig. 6. Volume storage density of hydrogen (1—the adsorbed and compressed gases; 2—the adsorbed phase) vs. temperature for wood-based carbon “WAC 3-00” (a), active carbon fiber “Busofit-M8” (b) and for different pressure: $P = 6$ MPa and 3.5 MPa.

sel (50 liters) the pressure varied from $P_0 = 6$ MPa down to $P_e = 0.1$ MPa. The steel vessel had the following geometrical characteristics: the length, 1.52 m; the outside radius, 0.1095 m; the thickness of the wall, 0.0065 m. The height of the finning disks was in line with the external boundary of the cylindrical sorbent layer. The radius of the heat pipe R_0 is 90 mm, and the radius of the outer sorbent layer is 91 mm. In the calculations, the parameters of the vessel were varied in the following ranges: rate of gas release, $0.15\text{--}0.7$ g sec $^{-1}$; thickness of the aluminum fin, 0.5–3 mm; step of finning, 20–30 mm. The data of the basic variant of calculation corresponded to wood-based carbon “WAC 3-00” $T_0 = 195$ K, $G = \pm 0.3$ g sec $^{-1}$, $\alpha_{\text{env}} = 3$ W m $^{-2}$ K $^{-1}$, $\alpha_s = \alpha_{\text{fs}} = 500$ W m $^{-2}$ K $^{-1}$, and $\alpha_f = 1000$ W m $^{-2}$ K $^{-1}$, $Q_{\text{hp}} = 500$ W.

The main characteristic of the vessel SSSG efficiency is the volume storage density ρ_v that represents the ratio of gas volume at normal conditions to the vessel volume. The second parameter—the dynamic coefficient of the vessel filling m (the latter represents the ratio of gas mass in vessel to its initial value), which is used in the process analyzing. Initially m is equal one. During the gas discharge m shows the fraction of nonrecoverable mass of gas $M_e \sim a(P_e, \bar{T}_e)$. Other characteristics of the process are the time of gas discharge (or charge), the mean-volume temperature of the sorbent bed \bar{T} , and the pressure in the vessel P .

Fig. 6 shows comparison between the total volumetric storage density and the adsorbed phase of hydrogen in the vessel in the interval of the ambient temperatures from 78 to 273 K. As indicated in the graphs it is necessary to take into account the presence of the compressed gas in the vessel, which fraction can be measured up to 30–50% at pressures 3.5–6 MPa. The initial hydrogen mass is determined from a condition of equilibrium. At temperature below 150 K the adsorbed volumetric storage density of hydrogen does not vary with the growth of pressure from 3.5 up to 6 MPa, the increase of stored hydrogen

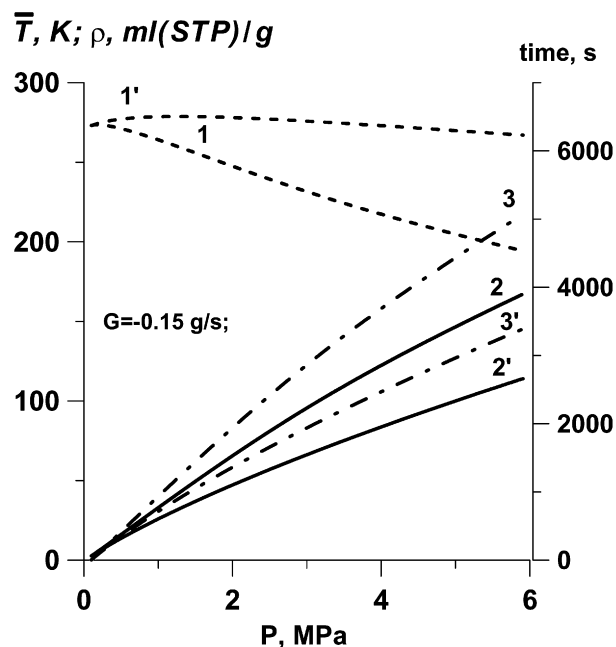


Fig. 7. The mean temperature of the sorbent (1, 1'), the volume storage density of hydrogen (2, 2') and the time of filling (3, 3'), vs. the pressure in the process of charge (filling) of the SSSG ($Q_{\text{hp}} = -500$ W: 1–3; $Q_{\text{hp}} = 0$ W: 1'–3').

occurs basically due to filling of meso- and macropores with the compressed gas. Following Fig. 6, for “Busofit” the maximum volumetric storage density of hydrogen at 77 K and 6 MPa was 380 ml(STP) ml $^{-1}$. As to mass characteristics, this system of storage is close to the qualifying standards of modern on-board systems, but it requires an application of advanced heat insulation. Both sorbents (the “Busofit-M8” and “WAC-3-00”) provide a volume storage density of 180 ml(STP) ml $^{-1}$ (3 wt%) at temperature 195 K, that allows to use a cheap heat insulation of the vessel (foamed polyurethane). However, the “WAC 3-00” sample ensured the value 120 ml(STP) ml $^{-1}$ at 273 K.

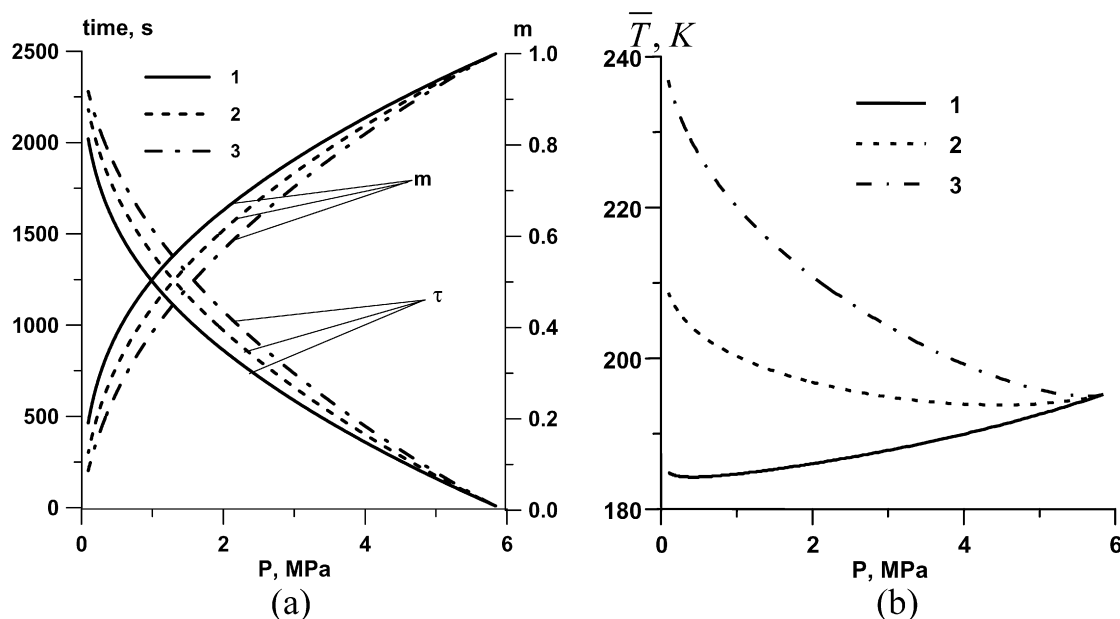


Fig. 8. The discharge time (a), dynamic coefficient of filling (a) and sorbent average temperature (b) vs. pressure in the SSSG for different additional heat flow applied by heat pipe: 1— $Q_{hp} = 0$ W; 2—500 W; 3—1000 W.

The process of hydrogen vessel filling through the reducer with a fixed rate of charge is an inverse problem to discharge of the vessel. In Fig. 7 the basic filling performances of a temperature-controlled vessel are shown. During the gas filling there is a rise of the pressure and temperature in the volume of sorbent, their variation being depending on the charge rate. A peculiarity of the designed storage system is the combination of heat transfer processes and accumulation of hydrogen in one volume. The rate of charge by hydrogen (time of filling) is determined by the reaction rate of gas absorption and heat transfer processes in a sorbent bed.

During the hydrogen consumption by the car engine the pressure in the vessel decreases from 6 MPa down to 0.1 MPa. In the technical gas storage application, only a part of the stored mass of hydrogen can be extracted from the vessel. This fraction of hydrogen is the gas mass reversibly stored/consumed during a charge-discharge cycle between the considered pressure levels. In the case of intensive extraction of gas, the percentage of its application can be decreased down to 50–60% due to the sorbent bed intensive cooling. An alternative to this is the gas heating procedure inside the sorbent bed with heat pipe heat exchanger. Fig. 8 shows the volume storage density of hydrogen, the mean temperature of the sorbent and the pressure change during the vessel gas discharge for three variants of sorbent bed heating conditions. In one variant, the influence of sorbent material heating is negligible. It was assumed, that heat transfer between the heat-pipe, the sorbent bed, and the fins (Fig. 1) is absent ($\alpha_s = \alpha_f = \alpha_{fs} = 0$). Thus, in the variant where the heat pipe was switched off, the sorbent bed thermally interacted only with the environment, while at all the remaining boundaries the heat flow was equal zero. The heat flow Q_{hp} increases the gas pressure and temperature inside the vessel. As temperature increases, the pressure in the cylinder during the

gas desorption decreases more slowly at the same gas flow rate. As a result, at $Q_{hp} = 1000$ W, the nonrecoverable gas mass decreases from 20 to 10%, as compared with the variant where the heat pipe is switched off (Fig. 8(a)). At Q_{hp} equal zero, the sorbent layer is cooled by 12 K (the endothermic reaction of gas desorption) below the initial temperature. An increase in the heating power ($Q_{hp} = 500$ W) makes it possible to release the gas from the cylinder more completely and ensure isothermal conditions of gas desorption. Finally, we can get a considerable reduction of hydrogen rest in the cylinder at pressure of 0.1 MPa.

In special cases (the increased gas output, Fig. 9) to provide maximum hydrogen extraction there is a necessity to select the optimal heating mode of sorbent material at the given environment temperature and the fixed gas rate. The abundant heat flow to the sorbent bed will result to excessive cylinder heating and the inadmissible increase of pressure. Fig. 10 illustrates the results of calculations to optimize conditions of the vessel heating (which ensures about 85% of the stored gas usage). At average flow rate $G = 0.3 \text{ g s}^{-1}$ and temperature $T_0 = 273 \text{ K}$ the additional heat flow $Q_{hp} = 300 \text{ W}$ is needed.

One of the goals of the present work was to investigate the influence of the kinetics of sorption on characteristics of cylindrical vessel filled with a sorbent material and gas. In available systems of gas storage, the deviation from the equilibrium state can be very high. The developed nonequilibrium model makes it possible to analyze the process of gas release from such systems. The transition to the equilibrium model corresponds to an infinitely large value of K_{s0} . Fig. 11 shows the dependences of the dynamic coefficient of the gas vessel filling m and the gas discharge time for different values of K_{s0} . At $K_{s0} = 0.6$, the infinitely fast reaction differs insignificantly from the ideal gas reaction. However, under other conditions, such an important

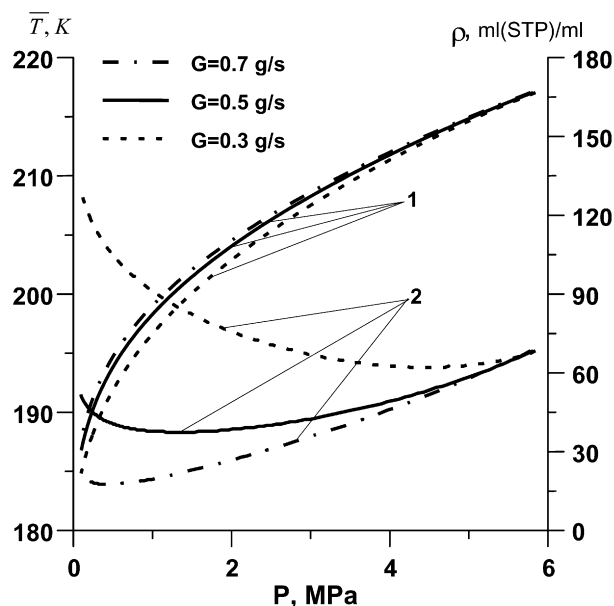


Fig. 9. The volume storage density of hydrogen (1), the mean temperature of the sorbent (2), vs. the pressure in the process of discharge of the SSSG for different gas flow rates.

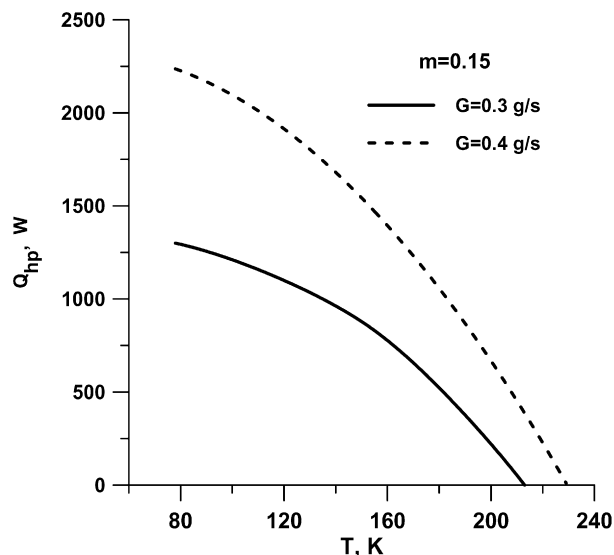


Fig. 10. The additional heat flux applied by heat pipe (at which the gas rest in the SGSS accounts for 15%) vs. an ambient temperature for different gas flow rates.

characteristic of the gas storage vessel as the nonrecoverable gas mass can be significantly worse when the kinetics is taken into account. The deviation from the thermodynamic equilibrium becomes more important for the sorbent material with the low thermal conductivity and high contact resistances to heat transfer.

4. Conclusions

- The designed sorption storage hydrogen system and modified sorbent materials (“Busofit-M8”, “WAC 3-00”) are promising for vehicles with internal combustion engine (es-

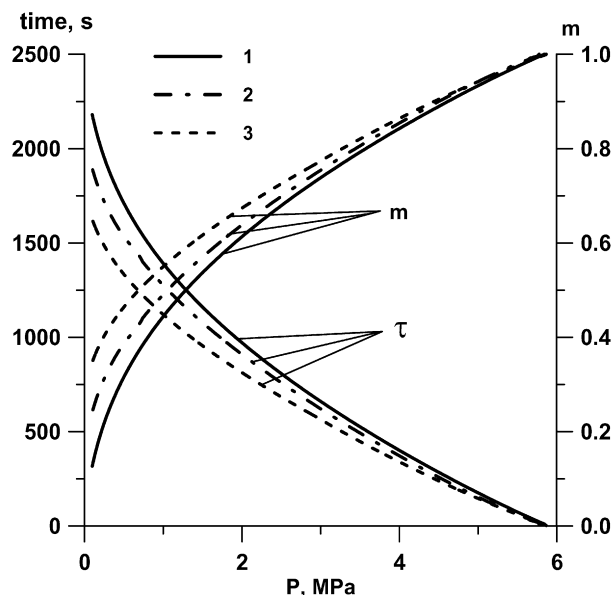


Fig. 11. Influence of allowance for the kinetics on the characteristics of the SSSG discharge ($G = 0.3 \text{ g sec}^{-1}$, $Q_{hp} = 500 \text{ W}$): 1—equilibrium model; 2— K_{s0} ; 3— $0.5K_{s0}$.

pecially for the dual-fuel automobile) and for the vehicles with fuel cells.

- Application of heat pipes as heat exchanger in the sorption storage systems of gas enables one to control the temperature distribution in the sorbent bed, influence the degree and time of gas extraction and provide an optimal operational regime.
- Numerical simulation of discharge and charge processes for hydrogen storage vessel filled with sorbent material was carried out at the range of temperatures from 77 up to 273 K and pressures interval 0–6 MPa. Calculation was performed with the use of mathematical model of heat, momentum and mass transfer processes in a cylindrical vessel with finned heat pipe. Nonstationary heat-balance equation takes into account heat of sorption and kinetic equation.

References

- [1] Basic Research Needs for the Hydrogen Economy, Report of the Basic Energy Sciences Workshop on Hydrogen Production, Storage, and Use, May 13–15, 2003.
- [2] C. Carpentis, A system consideration of alternative hydrogen storage facilities for estimation of storage costs, *Int. J. Hydrogen Energ.* 5 (1980) 423–437.
- [3] L. Schlapbach, A. Züttel, Hydrogen-storage materials for mobile applications, *Nature* 414 (2001) 353–358.
- [4] A.C. Dillon, M.J. Heben, Hydrogen storage using carbon adsorbents: past, present and future, *Appl. Phys. A: Materials Sci. Process.* A 72 (2001) 133–142.
- [5] J.J. Guilleminot, F. Meunier, J. Pakleza, Heat and mass transfer in a non-isothermal fixed bed solid adsorbent reactor: a uniform pressure—non-uniform temperature case, *Int. J. Heat Mass Transfer* 30 (1987) 1595–1605.

- [6] J.P. Barbosa Mota, E. Saatdjian, D. Tondeur, A.E. Rodrigues, A simulation model of a high-capacity methane adsorptive storage system, *Adsorption* 1 (1995) 17–27.
- [7] V.A. Babenko, L.E. Kanonchik, L.L. Vasiliev, Heat and Mass Transfer Intensification in Solid Sorption Systems, *J. Enh. Heat Transfer* 5 (1998) 111–125.
- [8] K. Inomata, K. Kanazawa, Y. Urabe, H. Hosono, T. Araki, Natural gas storage in activated carbon pellets without a binder, *Carbon* 40 (2002) 87–93.
- [9] M.M. Dubinin, The potential theory of adsorption of gases and vapors for sorbents with energetically nonuniform surfaces, *Chem. Rev.* 60 (1960) 235–241.
- [10] R.K. Agarwal, High pressure adsorption of pure gases on activated carbon: analysis of adsorption isotherms by application of potential theory and determination of heats and entropies of adsorption, PhD dissertation, Syracuse, 1988.
- [11] K.J. Chang, O. Talu, Behavior and performance of adsorptive natural gas storage cylinders during discharge, *Appl. Therm. Engrg.* 16 (1996) 359–374.
- [12] L.Z. Zhang, L. Wang, Performance estimation of an adsorption cooling system for automobile waste heat recovery, *Appl. Therm. Engrg.* 17 (1997) 1127–1139.
- [13] L.E. Kanonchik, V.A. Babenko, M.I. Rabetsky, Mathematical modeling of heat and mass transfer processes in adsorbed natural gas storage, in: *Proceedings of Non-Compression Refrigeration & Cooling (Int. Workshop 2)*, Odessa, Ukraine, 1999, pp. 94–99.
- [14] L.Z. Zhang, Design and testing of an automobile waste heat adsorption cooling system, *Appl. Therm. Engrg.* 20 (2000) 103–114.
- [15] N.V. Keltsev, *Basics of Adsorption Technology*, Himia, Moscow, 1976 (in Russian).
- [16] E. Gluckauf, Theory of chromatography: Formulas for diffusion into spheres and their application to chromatography, *Trans. Faraday Soc.* 51 (1955) 1540–1551.
- [17] A. Sakoda, M. Suzuki, Fundamental study on solar powered adsorption cooling system, *J. Chem. Engrg. Japan* 17 (1984) 52–57.
- [18] E.F. Passos, J.F. Escobedo, F. Meunier, Simulation of an intermittent adsorptive solar cooling system, *Solar Energy* 42 (1989) 103–111.
- [19] B.B. Saha, T. Kashiwagi, Performance evaluation of advanced adsorption cycle driven by near-environment temperature waste heat—comparison with conventional cycle, in: *Proceedings of Heat Pumping Technologies (International Energy Agency Conference 5)*, Toronto, Canada, 1996, pp. 277–284.
- [20] L.L. Vasiliev, L.E. Kanonchik, D.A. Mishkinis, M.I. Rabetsky, A new method of methane storage and transportation, *Int. J. Environmentally Conscious Design & Manufacturing* 9 (2000) 35–62.
- [21] D.M. Young, A.D. Growell, *Physical Adsorption of Gases*, L. Butterworth, 1962.
- [22] O. Zenkevich, *Method of Finite Elements in Engineering*, Mir, Moscow, 1975 (in Russian).
- [23] S. Hynek, W. Fuller, J. Bentley, Hydrogen storage by carbon sorption, *Int. J. Hydrogen Energy* 22 (1997) 601–610.
- [24] C. Carpentis, W. Peschka, A study on hydrogen storage by use of cryoadsorbents, *Int. J. Hydrogen Energy* 5 (1980) 539–554.
- [25] M.G. Nijkamp, J.E.M.J. Raaymakers, A.J. van Dillen, P.K. de Jong, Hydrogen storage using physisorption—materials demands, *Appl. Phys. A: Materials Sci. Process. A* 72 (2001) 619–623.
- [26] L.L. Vasiliev, A.G. Kulakov, D.A. Mishkinis, A.M. Safonova, N.K. Luneva, Activated carbon for gas adsorption, in: *Proceedings of Fullerene and Semifullerene Structures in the Condensed Media (Int. Symposium 3)*, Minsk, Belarus, 2004, pp. 110–115.